

Article

Fuel Gas Production from the Co-Gasification of Coal, Plastic Waste, and Wood in a Fluidized Bed Reactor: Effect of Gasifying Agent and Bed Material

Lucio Zaccariello *  and Maria Laura Mastellone

Department of Environmental, Biological and Pharmaceutical Sciences and Technologies, University of Campania, Via Antonio Vivaldi 43, 81100 Caserta, Italy; marialaura.mastellone@unicampania.it

* Correspondence: lucio.zaccariello@unicampania.it; Tel.: +39-0823-27-4657; Fax: +39-0823-27-4605

Abstract: In this study, the effect of gasifying agent and bed material on the performance of the co-gasification of a mixture of coal, plastic waste, and wood was investigated. The experimental runs were carried out in a lab-scale bubbling fluidized bed reactor utilizing air, oxygen-enriched air, a mixture of air and steam, and a mixture of oxygen and carbon dioxide as reactant gases, while silica sand, olivine, and a mixture of olivine and dolomite as bed materials were used. The results indicated that both gasifying agent and bed material strongly affect the gas composition and, as a consequence, the process performance. In particular, the test with oxygen-enriched air and silica sand provided a producer gas with the highest heating value (9.32 MJ/Nm³), while the best performance in terms of gas yield (2.98 Nm³/kg) and tar reduction (−94.5%) was obtained by utilizing the air/steam mixture and olivine. As regards tar composition, it was observed that the most abundant and recalcitrant tar substance groups are naphthalenes and PAHs. On the other hand, phenols and furans appear to be the most sensitive groups to the effect of gasifying agent and bed material.

Keywords: co-gasification; fuel gas; gasifying agent; bed material; tar composition



Citation: Zaccariello, L.; Mastellone, M.L. Fuel Gas Production from the Co-Gasification of Coal, Plastic Waste, and Wood in a Fluidized Bed Reactor: Effect of Gasifying Agent and Bed Material. *Sustainability* **2023**, *15*, 7547. <https://doi.org/10.3390/su15097547>

Academic Editors: Laura Vanoli, Simona Di Fraia and Fausto Arpino

Received: 24 March 2023

Revised: 22 April 2023

Accepted: 3 May 2023

Published: 4 May 2023



Copyright: © 2023 by the authors. Licensee MDPI, Basel, Switzerland. This article is an open access article distributed under the terms and conditions of the Creative Commons Attribution (CC BY) license (<https://creativecommons.org/licenses/by/4.0/>).

1. Introduction

Over the last decades, increasing efforts are being made to develop new alternative feedstocks for energy production due to fossil fuel depletion and the negative environmental impact related to their utilization. A promising direction is the development of an energy system based on the utilization of alternative feedstocks that allow reducing or shifting away from high-emission fossil fuels and highly efficient and environmentally friendly energy technologies [1].

Nowadays, coal is the most used fossil fuel for electric power generation. About 65% of the world's coal extraction is used for electricity production. It is also widely used for other industrial operations; for example, about 70% of steel plants use coal feedstock [2]. In 2019, global coal production was 7.9 billion tons. China is the world's biggest producer (46.6%), followed by India (9.7%), United States (8.1%), Indonesia (7.8%), Russia (5.3%), and the European Union (4.7%) [3]. The major disadvantage of coal utilization is its negative impact on the environment linked to the release of pollutants such as sulfur dioxide, carbon dioxide, heavy metals, etc. The environmental drawbacks related to coal utilization and its finite availability suggest preventing its use and replacing it with an alternative and/or renewable energy source.

The use of plastic waste feedstock can significantly reduce waste disposal concerns and produce fuels and electric power. In 2018, global plastics production reached about 360 million tons. A large part of this was produced in China (51%), North America (18%), and Europe (17%). In Europe, the largest end-use markets are packaging (40%), building and construction (20%), and the automotive industry (10%). Although the amount of plastic waste sent to recycling has greatly increased, 25% was still sent to landfill [4]. The large

availability and high energy content make plastic waste a promising feedstock for energy production [5]. However, plastics have a high fraction of volatile matter, low thermal conductivity, and a sticky nature. Hence, the utilization of plastic waste alone can result in operational difficulties due to its high flammability and agglomeration concerns [1].

Biomass represents, after coal, oil, and natural gas, the fourth largest energy source [6]. The use of biomass as feedstock for energy production reduces both the dependence on fossil fuels, considering their finite nature, and the net CO₂ emission, due to the utilization of biogenic carbon in the atmosphere by biomass growing through photosynthesis. Therefore, for these reasons, energy production from biomass can be considered renewable and neutral from a greenhouse gas (GHG) emission standpoint. On the other hand, using biomass alone may increase investment costs due to pre-processing operations (drying, size reduction, palletization, energy densification, etc.) and immature logistics for this feedstock [7]. In addition, for some biomasses, the uncertainty of their availability due to seasonal variations must be considered.

Several thermochemical processes have been developed (e.g., hydrothermal carbonization/liquefaction, torrefaction, pyrolysis, gasification, and combustion) to convert alternative fuels into thermal and electric energy, energy vectors, and chemicals [8–12]. Among these, the gasification process can offer increased possibilities for recovering valuable products from different feedstocks, ranging from clean fuel gas for energy recovery to bulk chemicals. In particular, it may use more efficient energy generation devices, such as gas engines and gas turbines, and therefore, it potentially has better electrical generation efficiencies. Fluidized bed gasification technology is one of the most promising due to its great operating flexibility: it is possible to operate the process with different feedstocks, gasifying agents, reactor temperatures, and gas residence times, to add reagents along the reactor freeboard and to operate with or without a specific catalyst as bed material [13–16]. On the other hand, gasification on a low-medium scale of some feedstocks, especially waste-derived fuels, is not yet a process of wide commercial application because of conversion efficiency losses and producer gas cleaning concerns. These concerns are related to the production of by-products such as char and tar.

Char represents the unconverted carbonaceous particles of the starting feedstock. Char can be easily separated from the producer gas through secondary methods, i.e., by using cyclones, scrubbers, fabric/ceramic filters, and electrostatic precipitators (secondary methods). On the other hand, massive char production generates consistent efficiency loss due to its high energy content.

Tar is a complex mixture of heavy hydrocarbons that condense at temperatures below 400 °C and represents the main technical obstacle of the gasification process. Tar can cause blockages in pipelines, valves, filters, heat exchangers, and other equipment. Tar content in the producer gas could exceed 100 g/Nm³, depending on the characteristics of the feedstock, the kind of gasifier, and the process operating conditions. However, some relevant applications of producer gas require a low tar content (lower than 100 mg/Nm³), as in the case of its utilization in gas engines, gas turbines, fuel cells, and catalytic reactors for producer gas upgrading [17]. As mentioned above, the formation of these by-products is strictly correlated to the fuel structure and composition. For example, the gasification of lignocellulosic biomass produces a large amount of char, while that of plastics generates a large amount of tar. This suggested the opportunity of investigating the simultaneous feeding of fuels with different characteristics since a possible synergy between products and intermediates generated by these feedstocks could improve the quality of the producer gas. Many studies reported positive synergistic effects during the co-gasification of two-component fuel mixtures among plastics, biomass, and coal compared to the mono-gasification of these feedstocks [18–20]. The main advantages reported are: (i) char generated from biomass or coal enhances the decomposition of the plastic polymer [21,22]; (ii) lower tar and char concentration in the gas [23,24]; (iii) higher gas yield [25]; (iv) increases in the carbon conversion and cold gas efficiencies [26]; and (v) reduced pollution emissions [27]. Moreover, a further non-negligible reason to develop the co-gasification process is the possibility of

extending the utilization of renewable energy sources and waste feedstocks to the existing coal gasifiers, thus reducing coal exploitation and overcoming biomass seasonal availability issues [28,29].

Even though many researchers studied the co-gasification of two-component fuel mixtures, very little research has been published exploring the co-gasification of three-component fuel mixtures of coal, plastic waste, and biomass. This three-component fuel mixture could further improve the co-gasification process performance because it produces more char, which plays a crucial role as a reaction intermediate in improving the process performance. Furthermore, although the effect of gasifying agent and bed material has been extensively investigated for mono-gasification and, to a lesser extent, for co-gasification of two-component fuel mixtures, there is a lack of information on the co-gasification of three-component fuel mixtures. The operating conditions of this process need to be investigated to a deeper extent, since the synergistic interactions among the three different fuel components could lead to different results from those obtained for the mono- and two-component gasification experiments. Hence, the aim of this work is to report the co-gasification potential of coal, plastic waste, and biomass in a bubbling fluidized bed gasifier as well as studying the influence of gasifying agent and bed material in process conversion and gas composition. The proportions of coal, plastic waste, and biomass in the co-gasification experiments were optimized in our previous study, where seven fuels with different proportions of coal, plastic waste, and wood were tested [30]. The results showed enhanced synergistic effects on the reduction in tar production when a fuel mixture composed of brown coal, recycled polyolefin plastics, and virgin wood in the ratio 5:3:2 was used. The enhanced synergistic effects on the reduction in tar concentration were attributed to the higher production of char, which played a crucial role as a reaction intermediate.

The experiments were carried out utilizing air, oxygen-enriched air, a mixture of air and steam, and a mixture of oxygen and carbon dioxide as gasifying agents. The role of bed material as an in situ catalyst was investigated by using silica sand, olivine, and a mixture of olivine and dolomite.

2. Experimental Apparatus and Procedure

2.1. Experimental Apparatus

The experimental runs were carried out using a lab-scale bubbling fluidized bed gasifier (BFBG) having a feeding capacity of 1–4 kg/h, depending on the type of fuel and operating conditions. A schematic illustration of the lab-scale gasifier is shown in Figure 1.

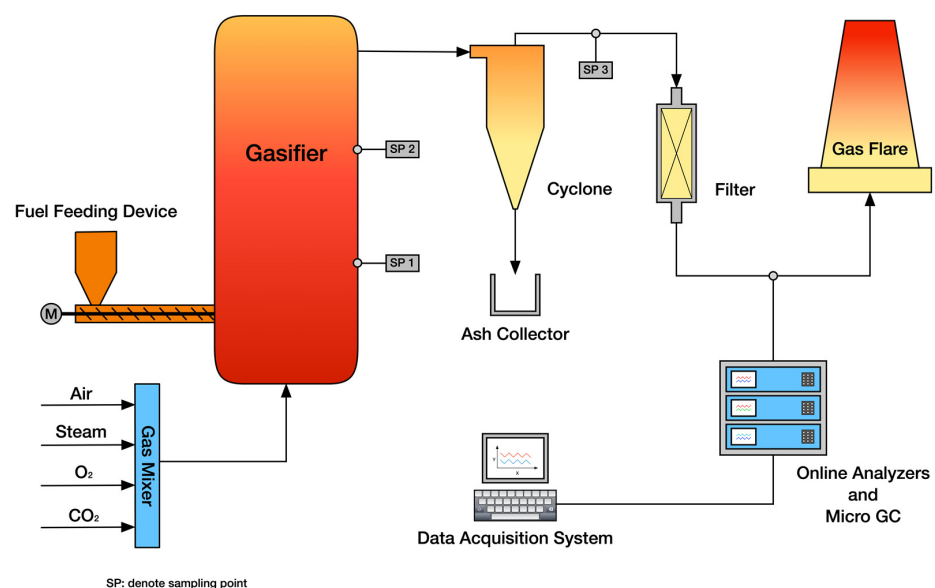


Figure 1. Schematic illustration of the lab-scale fluidized bed gasification apparatus.

The BFBG consists of a cylindrical column made of AISI 316L with a total height of 2.0 m (from the gas distributor plate to the product gas outlet) and an internal diameter of 0.10 m. The reactor is electrically heated by five shell furnaces equipped with a temperature controller that ensures the setting of the temperature of each reactor section (preheater, bed, and freeboard). The data provided by temperature and pressure sensors located at the key points of the experimental apparatus are recorded and monitored by a data acquisition system.

The gasifying agent is injected at the bed bottom through a distributor plate composed of three nozzles, specifically designed to ensure a homogeneous distribution of the fluidizing/gasifying gas in the bed cross-section. The feedstock is continuously over-bed fed using a screw-feeder device. A nitrogen flow of 0.20 Nm³/h is used to help the fuel feeding and to avoid the backflow of the hot gas to the feedstock hopper. At the reactor gas outlet, a gas cleaning section composed of a high-efficiency cyclone, a quartz wool filter, and a condenser provides elutriated particles and tar removal. Then, the gas is sent to a stack.

2.2. Analytical Equipment

The clean gas coming from the gas cleaning section was analyzed by using a four channels Agilent 3000 micro gas chromatograph (μ GC). Each channel was composed of a gas regulator, an injector, a column, and a TCD detector. In this study, the μ GC was operated with two channels. Channel 1 was equipped with a Molsieve 5 column, which provided the gas composition in terms of H₂, O₂, N₂, CH₄, and CO. Channel 2 was equipped with a PoraPlot Q column, which detected compounds such as CO₂ and light hydrocarbons, C₄H_m, i.e., hydrocarbons containing 2–4 atoms of carbon. Argon carrier gas was used for the Molsieve 5 column and helium for the PoraPlot Q column. The flow rate of producer gas was determined by using the tie component method applied to the nitrogen content in the dry producer gas.

Elutriated particles, consisting of char and fragmented bed particles, collected by the cyclone and particulate filter, were analyzed in a LECO TruSpec Elemental Analyzer to determine the content of carbon, hydrogen, nitrogen, and sulfur. The measurement method was based on the complete and instantaneous oxidation of the sample in a dual-stage furnace system operated at temperatures up to 950 °C. Pure oxygen was used to ensure the complete combustion of all the organic component of the samples and their conversion into gaseous products. The quantitative estimation of the gaseous products was obtained either by non-dispersive IR or thermal conductivity cells. In the CHN module, helium swept the combustion gas to separate infrared cells utilized for the detection of H₂O and CO. A thermal conductivity cell was used for the detection of N₂. As regards the S module, the sample was placed into a combustion boat and inserted in the furnace regulated at 1350 °C operated with pure oxygen. Sulfur evolved from the sample as SO₂. From the combustion system of the S module, the gases flowed to the CHN module, where an infrared cell was utilized for the detection of SO₂.

For the tar sampling, a system composed of a heated probe, a heated particle filter, and a series of five impinger bottles containing 50 mL of dichloromethane (DCM), was used. The sampler probe was inserted into a pipeline downstream of the reactor where the temperature of the producer gas was 400–450 °C. The gas sampling flow rate was set at 0.10 Nm³/h. The first two bottles were placed in a water bath at 20 °C, while the last three bottles were placed in a salt and ice bath at −15 °C so that the sampled gas is cooled in two steps. After the tar sampling, the content of the bottles was recovered and stored. Then, the bottles and the sampling line were rinsed three times with 500 mL of DCM. Both liquid fractions were mixed, filtered, and stored in dark bottles at 4 °C. The filters containing the solid particles were washed three times with 50 mL of DCM. The washing liquid was added to the previous sample to obtain a solution containing all the tar produced during the gasification test. Next, 5 mL of the tar sample was microfiltered and analyzed in a Perkin-Elmer Clarus 500 gas chromatograph coupled with a mass spectrometer (GC-MS). The oven temperature program started at an initial temperature of 45 °C and ended at

320 °C, with various temperature ramps and heating rates in between. The GC column was an Agilent DB-17MS with a total length of 30 m, an inner diameter of 250 µm, and a film thickness of 5 µm. For obtaining reliable experimental data, the sampling procedures of producer gas, elutriated particles, and tar were activated when the gas composition, temperature, and pressure were at steady state conditions and lasted for about 1 h.

2.3. Bed Materials

To evaluate the effect of active bed materials, the experimental tests were performed using silica sand, olivine, and a mixture of olivine (70%) and dolomite (30%) as bed materials. Silica sand is the inert reference material utilized to evaluate the performance of olivine and olivine/dolomite mixture as effective tar-removal bed additives. The main physical and hydrodynamic properties of the tested bed materials are reported in Table 1.

Table 1. Main physical and hydrodynamic properties of the bed materials tested.

Bed Material	Silica Sand	Olivine	Dolomite
Size range, µm	200–400	200–400	300–600
Sauter mean diameter, µm	300	280	330
Particle density, kg/m ³	2900	2600	2900
Minimum fluidization velocity ^a , m/s	0.030	0.025	0.038

^a Calculated in air at 850 °C.

2.4. Feedstock

Co-gasification tests were carried out using pellets composed of 50% brown coal, 30% recycled polyolefin plastics, and 20% virgin wood. The fuel pellets have a cylindrical shape, with a diameter of 6 mm and a length of about 20 mm (10–30 mm). Results of proximate and ultimate analyses of the feedstock utilized for the experimental runs are shown in Table 2.

Table 2. Main chemical properties of the tested fuel.

Proximate Analysis, % d.b.				Ultimate Analysis, % d.b.					Energy Content, MJ/kg	
VM	FC ^a	M	Ash	C	H	N	S	O ^a	HHV ^b	LHV ^c
68.92	19.14	4.11	7.83	62.28	8.11	0.19	0.13	17.35	30.61	25.71

VM = volatile matter. FC = fixed carbon. M = moisture. ^a Estimated by difference. ^b Evaluated according to Channiwala and Parikh [31]. ^c Calculated considering the latent heat of vaporization of the moisture and reaction water.

2.5. Experimental Data Processing

Data processing from feedstock characterization and on-line GC measurements used the following equations:

- Gas Specific Yield (GSY), defined as the ratio between the volumetric flow rate of the producer gas and the mass flow rate of the feedstock, was determined as follows:

$$GSY = \frac{Q_{\text{producer gas}}}{W_{\text{feedstock}}} \quad (1)$$

where Q and W indicate a volumetric and a mass flow rate, respectively. Q was determined by using the tie component method applied to the nitrogen content in the dry producer gas.

- Carbon Conversion Efficiency (CCE), defined as the ratio between the mass flow rate of the carbon contained in the final producer gas and the mass flow rate of carbon fed to the reactor through the feedstock, was determined as follows:

$$CCE = \frac{m_{\text{C,CO}_2} + m_{\text{C,CO}} + m_{\text{C,CH}_4} + m_{\text{C,C}_4\text{H}_m}}{m_{\text{C,feedstock}}} \quad (2)$$

where m_C is the carbon mass flow rates of the producer gas constituents (i.e., CO_2 , CO , CH_4 , and C_4H_m) and that of the feedstock. For run 4, CCE was calculated subtracting the carbon fed to the reactor with the CO_2 of the gasifying agent:

$$CCE = \frac{\Delta m_{C,\text{CO}_2} + m_{C,\text{CO}} + m_{C,\text{CH}_4} + m_{C,\text{C}_4\text{H}_m}}{m_{C,\text{feedstock}}} \quad (3)$$

with

$$\Delta m_{C,\text{CO}_2} = m_{C,\text{CO}_2}^{\text{OUT}} - m_{C,\text{CO}_2}^{\text{IN}} \quad (4)$$

where $m_{C,\text{CO}_2}^{\text{IN}}$ is the carbon fed to the reactor with the CO_2 of the gasifying agent and $m_{C,\text{CO}_2}^{\text{OUT}}$ is the carbon in the CO_2 contained in the producer gas at the exit of the reactor.

- Cold Gas Efficiency (CGE), defined as the ratio between the chemical energy of the producer gas generated during the gasification process and that entering to the system through the fuel, was determined as follows:

$$CGE = \frac{(Q \cdot \text{LHV})_{\text{producer gas}}}{(W \cdot \text{LHV})_{\text{feedstock}}} \quad (5)$$

where LHV is the lower heating value, while Q and W indicate a volumetric and a mass flow rate, respectively.

3. Results and Discussion

The effects of gasifying agent and bed material on the co-gasification of a mixture of coal, plastic waste, and wood were studied keeping fixed the fluidization velocity ($U_g = 0.4 \text{ m/s}$) and the equivalence ratio ($ER = 0.25$). To obtain useful information about the effect of the investigated parameters on the process autogenous temperature (T_{Bed}), the experimental runs were carried out in autothermal conditions, i.e., the temperature was established by the equilibrium between the endothermic and exothermic reactions which took place in the gasifier (without external heat sources).

The co-gasification test conducted using air and silica sand was chosen as a reference for evaluating the effect of the other gasifying agents and bed materials selected in this study. The operating conditions of the co-gasification tests are listed in Table 3.

Table 3. Operating conditions of the co-gasification tests conducted with an ER of 0.25.

Run	Gasifying Agent	Bed Material	T_{Bed}	W_{Fuel}	W_{Air}	W_{O_2}	W_{N_2}	W_{CO_2}	S/F
-	-	-	$^{\circ}\text{C}$	kg/h	kg/h	kg/h	kg/h	kg/h	-
1	Air	Silica sand	861	1.48	3.43	-	-	-	-
2	Enriched air	Silica sand	902	2.89	-	1.55	2.26	-	-
3	Air-Steam	Silica sand	846	1.24	2.75	-	-	-	0.50
4	Oxygen-Carbon dioxide	Silica sand	839	1.43	-	0.78	-	4.61	-
5	Air	Olivine	856	1.42	3.43	-	-	-	-
6	Air-Steam	Olivine	844	1.13	2.75	-	-	-	0.50
7	Air	Olivine/dolomite ^a	855	1.47	3.43	-	-	-	-
8	Air-Steam	Olivine/dolomite ^a	845	1.20	2.75	-	-	-	0.50

^a mixture composed of 70% olivine and 30% dolomite.

3.1. Effect of Gasifying Agent

To evaluate the effect of the gasifying agent on the gasification process performance, the results obtained during the test with air were compared with those resulting from the tests with oxygen-enriched air, a mixture of air and steam, and a mixture of oxygen and carbon dioxide as reactant gases. In these tests, a bed of silica sand was used. The main experimental results are reported in Table 4.

Table 4. Main results obtained from the co-gasification tests.

Items	Run 1	Run 2	Run 3	Run 4	Run 5	Run 6	Run 7	Run 8
Gas flow rate, Nm ³ /h	4.01	5.47	3.52	4.01	4.14	3.37	4.36	3.57
H ₂	7.52	14.41	11.08	5.57	9.39	10.65	10.88	12.74
CH ₄	3.90	6.45	3.93	3.98	4.45	4.35	4.96	3.99
CO	10.73	18.94	6.74	19.41	11.24	7.67	12.81	9.99
CO ₂	13.19	16.26	17.86	62.97	12.95	15.27	11.81	14.56
C ₄ H _m	3.25	4.87	3.31	3.03	2.46	3.05	3.01	2.42
N ₂	61.41	39.07	57.08	5.04	59.51	59.01	56.53	56.30
Gas specific yield, Nm ³ /kg	2.72	1.89	2.84	2.80	2.92	2.98	2.96	2.98
Lower heating value, MJ/Nm ³	5.61	9.32	5.61	6.51	5.63	5.71	6.49	5.69
Tar, g/h	7.11	5.45	0.59	1.20	0.82	0.33	0.51	0.72
Elutriate fines, g/h	50.16	230.90	60.34	70.27	48.11	35.86	134.40	124.21
Carbon conversion efficiency	0.86	0.89	0.90	0.89	0.88	0.88	0.94	0.90
Cold gas efficiency	0.59	0.69	0.62	0.71	0.64	0.66	0.75	0.66

The different concentration of the nitrogen inert gas in the tested gasifying medium gives a delusive effect in the evaluation of the actual extension of gasification reactions. Thus, to avoid this inconvenience the gas composition on a dry and inert-free basis was reported. Gas specific yield (GSY), lower heating value (LHV), carbon conversion efficiency (CCE), and cold gas efficiency (CGE) were, instead, calculated considering the producer gas on dry basis and the feedstock as it is. Regarding run 4, where a mixture of oxygen and carbon dioxide as gasifying agent was used, the gas composition was reported on a nitrogen (purge nitrogen)-free basis and normalized with respect to the carbon dioxide feed to the reactor with the gasifying agent. For this run, CCE was calculated by subtracting the carbon content entering the process through the gasifying agent from the producer gas.

3.1.1. Effect of Oxygen-Enriched Air

The utilization of a gasifying agent having an increased content of oxygen was studied by comparing the results obtained from the tests with air (reference test) and oxygen-enriched air by keeping fixed the ER and the U_g.

The results showed that one of the main effects of the higher oxygen concentration, and the corresponding decrease in nitrogen amount in the reactant gas, was the increase in bed temperature. In particular, the temperature increased from 861 to 902 °C as the oxygen concentration changed from 21 to 38%. This result was due to the combined effect of the great extension of the oxidation reactions (R1–3), promoted by the higher oxygen concentration and the less marked role of temperature moderator played by nitrogen as a result of its lower concentration in the gasifying agent:

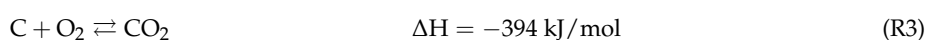
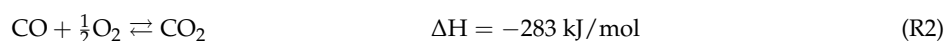
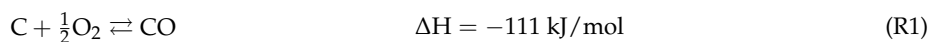


Figure 2 shows an increase in CO (+11.8%) and a decrease in CO₂ (−21.9%) concentrations. The marked decrease in CO₂ content may be explained by referring to the larger extension of the reaction between C-char (carbon contained in the char) and CO₂ (Boudouard reaction, R4), which was favored by the elevated reactor temperature.

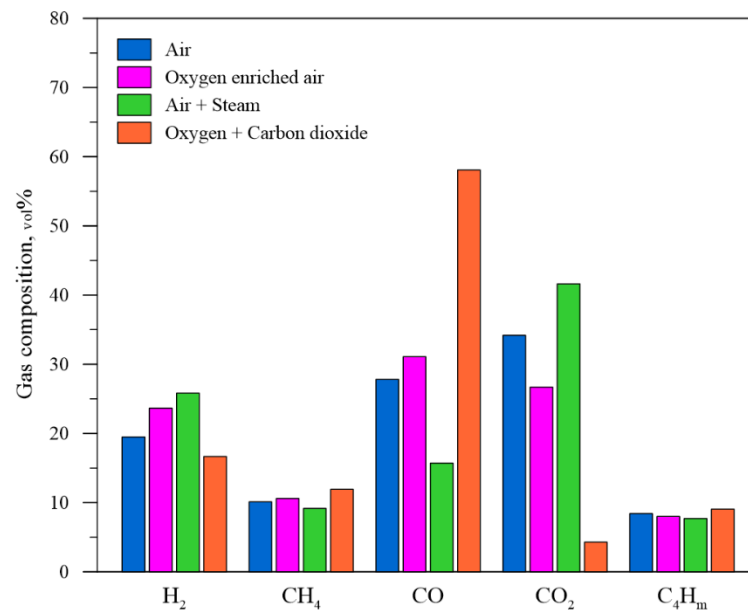
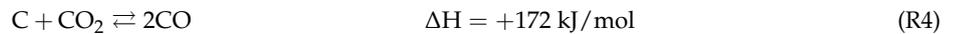


Figure 2. Effect of gasifying agent on gas composition obtained during the co-gasification tests with a bed of quartz sand. Gas composition is presented on dry inert basis and normalized with respect to the carbon dioxide feed to the reactor with the gasifying agent.

The higher reaction temperature did not significantly affect the concentrations of CH₄ and C₄H_m in the producer gas as they remained almost unchanged (+4.7%, for CH₄; −5.1%, for C₄H_m).



Similar results were obtained by Han et al. [32] by raising the bed temperature from 600 to 900 °C during the air gasification of SFR in a bubbling fluidized bed reactor. The authors observed an increase in H₂, CO, CH₄, and C₂ hydrocarbons content, and a decrease in CO₂ and C₃ hydrocarbons concentration. They also reported a drastic decrease in tar production (about 67%) when the bed temperature was raised from 600 to 900 °C.

The unvaried concentration of CH₄ and C₄H_m could be explained considering the opposite effect of the fuel thermal cracking and hydrocarbons polymerization reactions. To a large extent, both CH₄ and C₄H_m were generated during the pyrolysis step of the gasification process. Therefore, a higher reaction temperature favored the production of CH₄ and C₄H_m as a consequence of the more intense thermal cracking of the feedstock. On the other hand, light hydrocarbons decreased as they were involved in the polymerization reactions of heavy hydrocarbons (tar) [33].

As mentioned, a higher reactor temperature supports the thermal carbonization of heavy hydrocarbons. This process involves dehydrogenation and polymerization reactions that lead to the production of hydrogen and solid polycondensed aromatic molecules (soot) with a high C/H ratio (R5,6):



where C_xH_y represents tar and C_nH_m represents hydrocarbons with a smaller carbon number than C_xH_y.

This hypothesis, as can be deduced from Figures 2 and 3, is supported by the increase in H₂ concentration (+21.4%), the simultaneous reduction in tar production (−43.8%), and the increase in carbon content in the elutriated fines collected by the cyclone at the reactor exit (+215.2%) gasification tests with a bed of quartz sand.

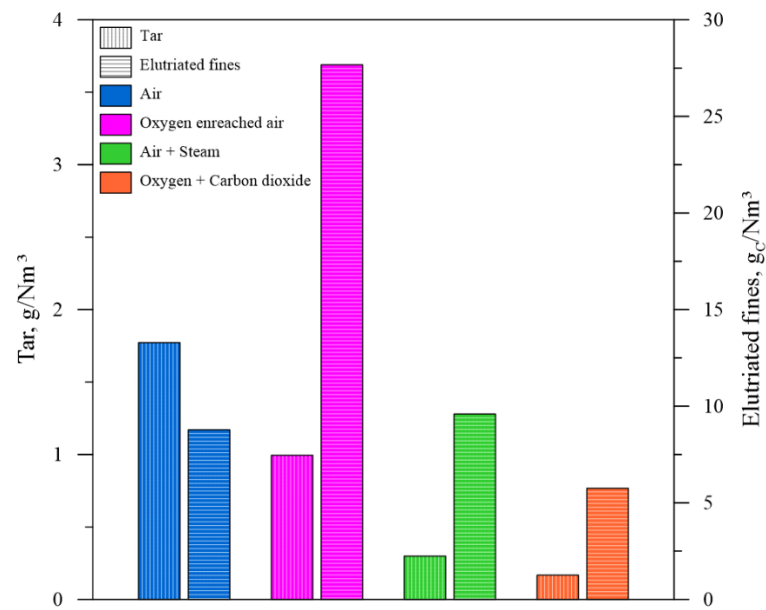


Figure 3. Effect of gasifying agent on tar and elutriated fines carbon content obtained during the co-gasification tests with a bed of quartz sand.

Due to the reduced amount of nitrogen in the gasifying agent, GSY decreased about 30% (Figure 4A). On the other hand, the LHV of producer gas greatly increased (+66.1%) due to the higher concentration of gaseous compounds with greater chemical energy content (Figure 4B).

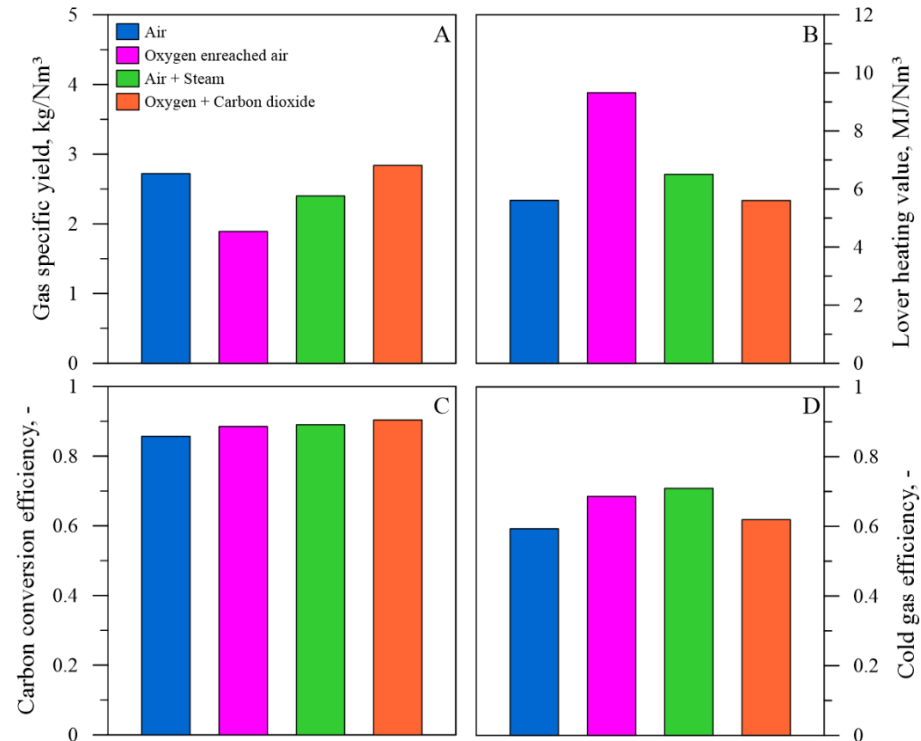


Figure 4. Effect of gasifying agent on specific yield (A), heating value (B), carbon conversion efficiency (C), and cold gas efficiency (D) of gas obtained during the co-gasification tests with a bed of quartz sand.

The higher reaction temperature promoted the extension of gasification reactions and the thermal cracking of tar into permanent gas, which resulted in an increase in either CCE, from 85.7% to 88.5%, and CGE, from 59.3% to 68.6% (Figure 4C,D).

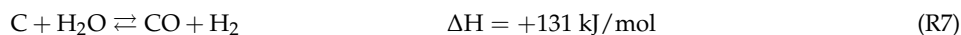
3.1.2. Effect of Steam

Steam gasification is one of the most effective processes of generating a high syngas quality from carbonaceous feedstocks. However, the process is endothermic and thus could require a more complex design for heat supply [34]. A possible simple solution to overcome this issue is represented by the addition of some amount of oxygen in the gasifying gas. It allows the development of oxidation reactions that provide the necessary heat to carry out the process in autothermal conditions, therefore avoiding complicated design solutions and investment costs.

In this study, the effect of steam addition to an air stream, providing a fixed value of ER, was investigated by comparing the results obtained in runs 1 and 3.

Figure 2 reveals that the addition of steam determined an increase in H₂ (+32.5%) and CO₂ (+21.7%) and a decrease in CO (−43.5%) concentrations. Steam addition slightly affected the production of CH₄ and C₄H_m, which moderately decreased (−9.4% for CH₄ and −8.4% for C₄H_m). These results can be explained by considering the reactions R7–11.

On the one hand, steam addition enhanced the water-gas (R7) and hydrocarbons steam reforming reactions (R8–10) and thus the formation of H₂ and CO (and the decrease in the contents of both CH₄ and C₄H_m). On the other hand, the results indicated the predominant role of the water-gas shift reaction (R11), which led to the reduction in CO and the increase in CO₂ and H₂ in the producer gas:



One of the most significant effects of steam addition is the considerable reduction in tar and carbonaceous particles. The use of steam produced an impressive conversion of tar that reduced by 90.6% (R10), while the carbon content in the elutriated fines decreased by 34.4% (R7). As a result, the conversion of tar and C-char of elutriated fines into permanent gas resulted in an increase in GSY (+4.4%) and CCE (+5.5%). Meanwhile, LHV and CGE remained almost unchanged due to the opposite effect of H₂ and GSY increase and CO and light hydrocarbons reduction.

3.1.3. Effect of Carbon Dioxide

The utilization of carbon dioxide as a gasifying medium is promising since tar and char could be converted into permanent gas, improving the gasification process performance [35–37]. However, the utilization of carbon dioxide establishes an intensive endothermic process, which requires a specific reactor design or the addition of oxygen to promote oxidation reactions that provide the necessary thermal energy to support the exothermic reactions of the gasification process. In this investigation, the thermal energy needed to develop the gasification process in autothermal conditions was obtained by the addition of oxygen, which promotes oxidation reactions. The results of CO₂ gasification were compared with those obtained with only air (run 1 versus run 4).

Comparing the reactor CO₂ inlet and outlet flow rates, a positive difference was observed (+0.18 Nm³/h), indicating that additional CO₂ was produced. The further generation of CO₂ (+4.29%) was mainly due to the oxidation reactions occurred between the oxygen contained in the gasification medium and the pyrolysis products (char and volatiles) generated during the first step of fuel degradation inside the reactor. Figure 2

shows that CO₂ gasification led to an impressive increase in CO content (+109%). This can be attributed to the larger extension of the Boudouard reaction (R4). The concentration of CH₄ and C₄H_m increased to a lesser extent (+17.82 and +7.64%, respectively). On the other hand, a reduction in H₂ (−14.49%) was observed. The increase in light hydrocarbons and the simultaneous reduction in H₂ concentrations could indicate a limited conversion of light hydrocarbons by the dry reforming reaction (R12). This may be attributed to the not very high reaction temperature (see Table 3):



Pinto et al. [38] studied the effect of the gasifying agent on bubbling the fluidized bed co-gasification of a mixture of waste rice biomass and polyethylene. They observed an increase in CO production with increasing contents of CO₂ in the gasifying agent. The Authors attributed the high production of CO to the larger extension of the Boudouard reaction. In addition, the results displayed no great variation in H₂ and CH₄ concentrations and a decrease in light hydrocarbons due to their conversion through dry reforming reactions. In addition, Cheng et al. [39] reported that a high concentration of CO₂ promotes the reverse of the water gas shift reaction. These findings could explain the huge increase in CO and the reduction in H₂ in the producer gas observed in run 4.

The main advantage of using carbon dioxide as a gasifying agent was the impressive reduction in tar. In fact, Figure 3 shows that tar concentration was reduced by about 83%. This drastic tar reduction can be attributed to its conversion through the dry reforming reaction (R13). The results indicate that CO₂ gasification produced intensive destruction of tar and that, in these specific operating conditions, dry reforming reactions were not sufficiently developed to perform an intensive conversion of light hydrocarbons into CO and H₂:



Figure 3 shows that the carbon content of elutriated fines in the tests with the mixture of oxygen/carbon dioxide increased, which appears to be in contrast with the effect of the development of the Boudouard reaction. This phenomenon could be explained by considering that the Boudouard reaction is slower than the oxidation reaction of C-char.

As shown in Figure 4, the utilization of the more reactive gasifying agent enhanced the tar reforming reactions which, in turn, had a favorable effect on the gas quality, increasing GSY (+3.0%), LHV (+16.0%), CCE (+3.9%) and CGE (+19.6%).

3.2. Effect of Bed Material

Among all the natural bed materials used as in situ catalysts during the gasification process, olivine (a magnesium–iron silicate) and dolomite (a calcium–magnesium carbonate) are expected to be very effective in improving the producer gas quality. In this section, experimental runs 1, 5, and 7 are compared to evaluate the effect of olivine and a mixture of olivine and dolomite on the performance of the gasification process.

3.2.1. Effect of Olivine

The results showed that the utilization of olivine as bed material produced a significant change in gas composition (Figure 5). It can be observed an increase in H₂ (+19.0%) and CH₄ (+8.8%) concentrations in the tests with olivine when compared to the use of silica sand. On the other hand, a decrease in CO₂ (−6.4%) and C₄H_m (−27.9%) was detected. Meanwhile, the concentration of CO remained substantially unchanged.

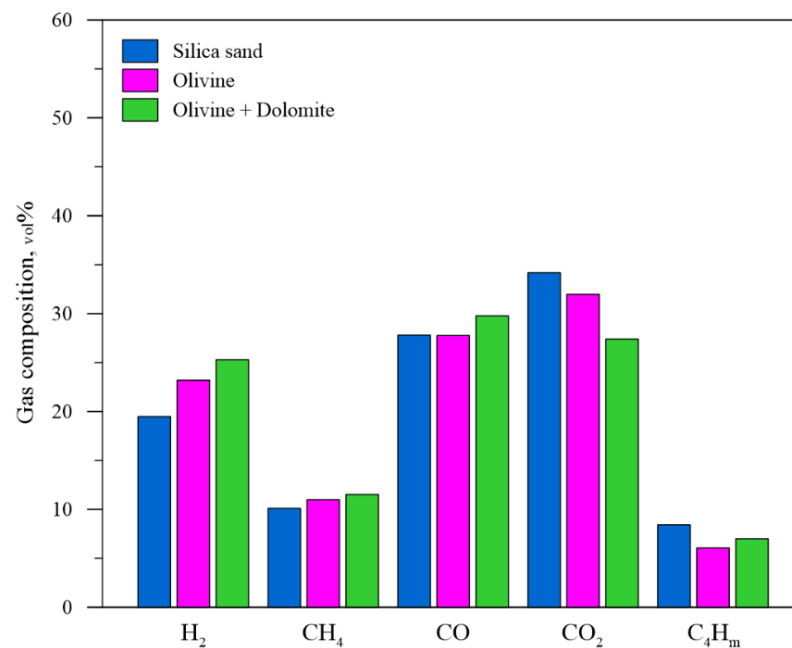


Figure 5. Effect of bed material on gas composition obtained during the co-gasification tests with air as gasifying agent. Gas composition is reported on dry inert basis.

The use of olivine improved the performance of the gasification process by promoting catalytic reactions that enhanced the reforming of tar into permanent gas (R14, 15). The great extension of these reactions during the co-gasification test with olivine was highlighted by a decrease of 88.9% in tar concentration (Figure 6). At the same time, an increase in GSY (+7.6%) was observed (Figure 7A). The increase in CCE and CGE values further demonstrates the effectiveness of olivine as a bed additive. The results indicated that CCE increased from 85.7% to 87.7% and that CGE moved from 59.3% to 64.0% as a direct consequence of the catalytic cracking of tar produced by olivine particles (Figure 7C,D).

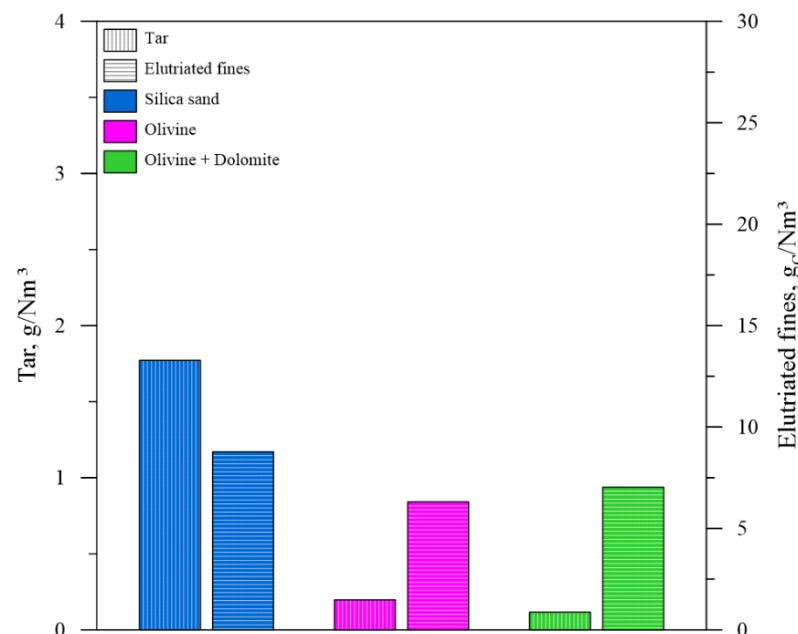


Figure 6. Effect of bed material on tar and elutriated fines carbon content obtained during the co-gasification tests with air as gasifying agent.

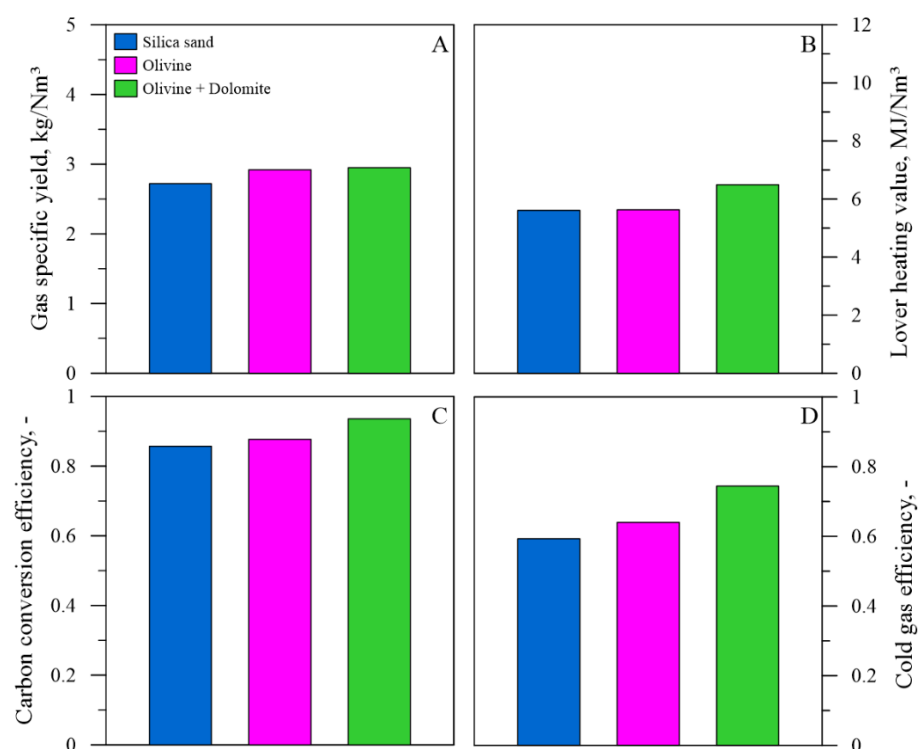


Figure 7. Effect of bed material on specific gas yield (A), heating value (B), carbon conversion efficiency (C), and cold gas efficiency (D) of gas obtained during the co-gasification tests with air as gasifying agent.

Comparable results were obtained by Mastellone and Zaccariello [40] during the air gasification of plastic waste in a pilot-scale bubbling fluidized bed reactor. They reported a strong increase in H_2 and CO as well as a reduction in CO_2 , CH_4 , and light hydrocarbons when olivine was used instead silica sand. Moreover, the authors also observed an impressive tar reduction and an enhancement of carbon conversion efficiency.

3.2.2. Effect of Olivine/Dolomite Mixture

The producer gas obtained during the test with the olivine/dolomite mixture displayed higher concentrations of H_2 and CH_4 and a lower amount of CO_2 than those found in the tests with silica sand and olivine. Instead, C_4H_m concentration was about halfway between the values obtained with silica sand and olivine (Figure 5). The great advantage due to the use of olivine/dolomite mixture was shown by the impressive reduction in tar concentration in the producer gas, which decreased about 94% (Figure 6). The positive effect of tar reforming was reflected in the increase in yield and calorific value of producer gas, which rose 8.9% and 15.7%, respectively (Figure 7A,B). Figure 7C,D shows that CCE (+10.0%) and CGE (+26.0%) also improved.

In contrast to the significant advantages of dolomite addition to the bed material, a drastic increase in fine particles production was observed: the elutriated fines collected by the cyclone in the run with silica sand increased from 50.2 to 134.4 g/h in the run with olivine/dolomite (Table 4). This was determined by the breakdown of dolomite particles inside the fluidized bed, which led to a remarkable carryover of fines from the reactor.

The utilization of olivine/dolomite mixture as a bed material produced similar effects on the producer gas composition to those observed in the co-gasification test with pure olivine, although some differences may be marked. It is recognized that iron, magnesium, and calcium, largely present in olivine (iron and magnesium) and dolomite (magnesium, calcium, and lower amount of iron) particles, catalytically enhance the tar reforming reactions (R14, 15). In particular, the results indicated that iron catalytically assisted the dehydrogenation and carbonization reactions, while magnesium and calcium improved the

dehydrogenation and isomerization reactions of heavy hydrocarbon fragments produced by the thermal cracking of the feedstock:



where C_xH_y represents tar and C_nH_m represents hydrocarbons with a smaller carbon number than C_xH_y .

The result of the enhancement of these reactions, as above mentioned, was the production of a producer gas with an almost complete absence of tar and with a higher concentration of hydrogen and methane, whereas light hydrocarbons showed concentrations about halfway between those obtained with silica sand and olivine. This suggests that the catalytic support to the cracking and isomerization was active so that tar molecules were cracked, and hydrogen and light hydrocarbons were formed. On the other hand, the dehydrogenation and carbonization reactions, due to the catalytic activity of iron oxides, appeared inhibited considering the higher concentration of tar and intermediate values of hydrogen, methane, and light hydrocarbons obtained during the test with a bed of pure olivine. Similar results were obtained by Arena et al. [41], who studied the effect of bed material during the gasification of waste-derived fuels in a pilot-scale bubbling fluidized bed reactor. The authors demonstrated that the catalytic action determined by magnesium oxide is almost completely developed. On the contrary, the catalytic activity of the iron oxides is repressed by the presence in the waste-derived fuels of ferrous and non-ferrous competing metals, poisoning elements, and a large amount of oxygen.

3.3. Combined Effect of Gasifying Agent/Bed Material

The performed co-gasification tests allowed the evaluation of the combined effect gasifying agent/bed material. The results revealed that steam addition greatly improved the performance of the co-gasification process when combined with the tested bed materials. Comparing tests 4, 6, and 8, it can be observed that the test with air-steam/olivine showed intermediate values of H_2 , CO , CO_2 , and C_4H_m , and higher values of CH_4 compared to those obtained in the tests with air-steam/silica sand and air-steam/olivine-dolomite. The combination of air-steam/olivine gave the best results in terms of tar reduction: only 0.097 g/Nm^3 of tar was produced. This means that a reduction of 94.5% was achieved by relating this result to the tar concentration obtained in the reference test (air/silica sand). Moreover, negligible variations in GSY, LHV, and CGE, were observed, even though the tests with beds of olivine and olivine-dolomite displayed slightly better performance than those obtained in the test with silica sand. Considering the combined effect of gasifying agent/bed material on tar production, it should be highlighted that the tests with air-steam/olivine-dolomite showed worse performance than using only air as a gasifying agent and olivine-dolomite mixture as bed material. These results seem to indicate that the catalytic action of dolomite was inhibited by the presence of steam in the gasifying agent.

3.4. Tar Composition

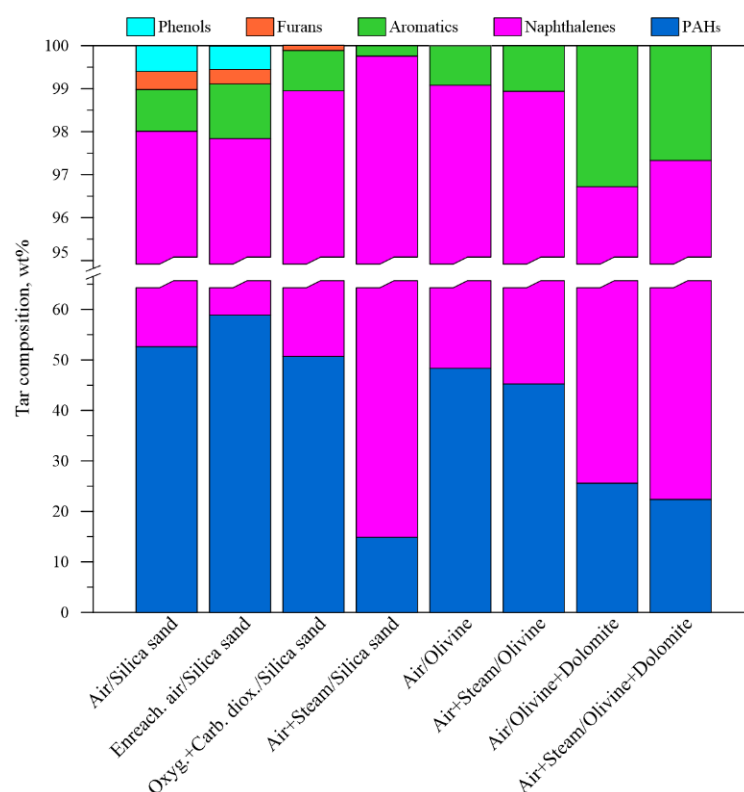
A further significant aspect that should be considered to optimize the gasification process, in addition to the determination of the total tar production, is the definition of tar composition that could address the configuration of the gas cleaning section [42].

For a more accurate understanding of the tar evolution caused by the utilization of the different gasifying agents and bed materials, a total of 42 individual tar components were quantified by GC–MS analysis. These compounds, for easier comparison, were grouped considering their chemical similarity in the following substance groups: phenols, furans, aromatics, naphthalenes, and PAHs. Table 5 reports the compounds constituting each tar group.

Table 5. Groups and substances of tars.

Group	Substance
Phenols	phenol, cresol, 3-Methylphenol, 4-Methylphenol.
Furans	benzofuran, and dibenzofuran.
Aromatics	benzotrinitril, phenylacetylene, styrene, and toluene.
Naphthalenes	naphthalene, 1-methylnaphthalene, and 2-methylnaphthalene.
PAHs	acenaphthene, acenaphthylene, acephenanthrylene, anthracene, benz[a]anthracene, benzo[b]fluoranthene, benzo[ghi]fluoranthene, benzo[j]fluoranthene, benzo[k]fluoranthene, benzo[c]phenanthrene, benzo[a]pyrene, benzo[e]pyrene, benzo[ghi]perylene, biphenyl, biphenylene, chrysene, coronene, cyclopenta[def]phenanthrene, cyclopenta[cd]pyrene, dibenz[a,h]anthracene, dibenzo[a,i]pyrene, fluoranthene, fluorene, indane, indene, indeno [1,2,3-cd]pyrene, perylene, phenanthrene, and pyrene.

Figure 8 reveals that the most abundant tar substance groups quantified by GC–MS analysis in the tar samples were naphthalenes (which range from 38.81%, run 2, to 81.59%, run 4) and PAHs (varying from 16.09%, run 4, to 58.96%, run 2). Instead, lower amounts of light tar as aromatics (from 0.68%, run 5, to 3.28%, run 7), phenols (undetected in runs 3–8, up to 0.59%, in run 1), and furans (undetected in the runs 4–8, up to 0.41%, in run 1), were found.

**Figure 8.** Effect of gasifying agent and bed material on tar composition obtained during the co-gasification tests.

During the tests with silica sand (run 1 vs. runs 3 and 4), the utilization of steam and CO₂ reduced PAHs and increased naphthalenes fractions. On the other hand, oxygen-enriched air had an inverse effect, i.e., it increased PAHs and reduced naphthalenes (run 1 vs. run 2).

Comparing the tests with air and steam utilizing beds of olivine and olivine/dolomite mixture, a reduction in PAHs and an increase in naphthalenes was observed. Thus, it can be argued that steam and CO₂, as a gasifying agent, and olivine and olivine/dolomite,

as bed materials, repressed the polymerization reactions and/or favored the cracking of heavy tar. In particular, the results indicated that CO₂ and dolomite produced more intense cracking of PAHs than steam and olivine. The test performed with CO₂ showed the lowest fraction of PAHs (16.09%), followed by the tests with olivine/dolomite (25.59%, with air, and 22.37%, with steam) and with only olivine (48.43%, with air, and 45.92%, with steam).

Phenols and furans appeared to be the most sensitive groups to the effect of the utilized gasifying agents and bed materials. Phenols were only found in runs 1 and 2, while furans were detected in runs 1–3. A possible explanation is that the hydroxyl and ether functional groups make phenols and furans more reactive, thus favoring condensation and/or ring-opening reactions. These results are consistent with those found by Abu El-Rub et al. [43], who used different gasifying agents and bed materials to remove phenol, as a tar compound model, from a synthetic gas. The authors reported that during the steam and dry reforming experiments, phenol conversion was more than 97% at 800 °C and more than 98% at 900 °C. Instead, the catalytic experiments showed phenol conversion of 34.5, 42.7, and 90.0% at 700 °C for beds of silica sand, olivine, and dolomite, respectively, and a conversion of 100% at 900 °C with all these bed materials. The aromatics group was detected in all experimental tests with an increased concentration in the runs conducted with a bed of olivine/dolomite mixture (runs 7 and 8). Lower amounts of this group were detected in the tests with only olivine (runs 5 and 6).

Regarding the individual tar components, naphthalene was by far the most abundant compound, accounting for 35.04% (run 2) and 79.76% (run 4) of the total tar production, whereas indene (up to 25.67%), acenaphthylene (up to 16.13%), phenanthrene (up to 14.47%), pyrene (up to 6.26%), fluoranthene (up to 6.07%), fluorene (up to 3.32%) and anthracene (up to 3.28%) were the main representatives of the PAHs group. The predominant elements of the aromatics, phenols, and furans groups were styrene, phenol, and dibenzofuran, which in all cases, contributed less than 3% of the total tar amount.

4. Conclusions

A lab-scale BFB reactor was used to investigate the effect of gasifying agent and bed material on the performance of the co-gasification process of coal, plastic waste, and wood.

The results indicated that the test with oxygen-enriched air provided a gas with the highest LHV (9.3 MJ/Nm³) and a satisfying CGE (68.6%). At the same time, it exhibited poor performance in terms of tar reduction (−23.3%), high carbon loss through the elutriated fines (+215.2%), and low gas yield (1.89 Nm³/kg). Steam addition caused a drastic tar reduction (−91.7%) and showed a reduced loss of carbon through the elutriated fines (−34.4%), an acceptable LHV (5.6 MJ/Nm³), and a high gas yield (2.8 Nm³/kg) as well as CCE (90.4%). The test with the mixture of oxygen/carbon dioxide displayed intermediate results between those obtained with oxygen-enriched air and the mixture of air/steam.

The type of bed material greatly affected the performance of the co-gasification process. The best results in terms of tar reduction (−92.9%), gas yield (2.95 Nm³/kg), LHV (6.5 MJ/Nm³), CCE (93.6%), and CGE (74.4%) were obtained by utilizing the mixture of olivine/dolomite as bed material. On the other hand, the utilization of this bed material determined by far the highest production of solid particles in the gas (30.9 g/Nm³).

As regards the combined effect of gasifying agent/bed material, the combination air-steam/olivine provided the absolute best results in terms of tar reduction. In this test, only 0.097 g/Nm³ of tar was produced.

For all the co-gasification tests, it was observed that the most abundant and recalcitrant tar substance groups were naphthalenes (up to 81.6%) and PAHs (up to 59.0%). Instead, lower amounts of aromatics (up to 3.3%), phenols (up to 0.6%), and furans (up to 0.4%) were found.

Based on the obtained results, the best option to produce a gas suitable for utilization in efficient end-user devices for energy production from the co-gasification of coal, plastic

waste, and wood could be the use of a mixture composed of air and steam or air, oxygen, and steam as gasifying agent and olivine as bed material.

Author Contributions: Conceptualization, L.Z. and M.L.M.; Methodology, L.Z. and M.L.M.; Validation, L.Z. and M.L.M.; Investigation, L.Z.; Data curation, L.Z. and M.L.M.; Writing—original draft, L.Z. and M.L.M.; Writing—review & editing, L.Z. and M.L.M.; Visualization, L.Z. and M.L.M.; Funding acquisition, M.L.M. All authors have read and agreed to the published version of the manuscript.

Funding: This research received no external funding.

Acknowledgments: The authors are indebted to Ansaldo Ricerche S.p.A., which financially supported part of the experimental activities.

Conflicts of Interest: The authors declare no conflict of interest.

Nomenclature

CCE	Carbon conversion efficiency	[-]
CGE	Cold gas efficiency	[-]
ER	Air-to-fuel equivalence ratio	[-]
GSY	Gas specific yield	[Nm ³ /kg]
HHV	Higher heating value	[MJ/kg]
LHV	Lower heating value	[MJ/Nm ³ or MJ/kg]
Q	Volumetric flow rate	[Nm ³ /h]
S/F	Steam/fuel ratio (at the gasifier inlet)	[-]
T _{Bed}	Fluidized bed temperature	[°C]
U _g	Superficial gas velocity (at the gasifier inlet)	[m/s]
W	Mass flow rate	[kg/h]
W _{Air}	Mass flow rate of air (at the gasifier inlet)	[kg/h]
W _{CO2}	Mass flow rate of carbon dioxide (at the gasifier inlet)	[kg/h]
W _{Fuel}	Mass flow rate of carbon dioxide (at the gasifier inlet)	[kg/h]
W _{N2}	Mass flow rate of fuel (at the gasifier inlet)	[kg/h]
W _{O2}	Mass flow rate of oxygen (at the gasifier inlet)	[kg/h]

References

- Fazil, A.; Kumar, S.; Mahajani, S.M. Downdraft co-gasification of high ash biomass and plastics. *Energy* **2022**, *243*, 123055. [CrossRef]
- Holuszko, M.E.; de Klerk, A. Coal Processing and Use for Power Generation. In *Future Energy*, 2nd ed.; Letcher, T.M., Ed.; Elsevier: Amsterdam, The Netherlands, 2014; pp. 53–73.
- Available online: <https://www.iea.org/data-and-statistics/charts/world-total-coal-production-1971-2020> (accessed on 20 February 2022).
- Available online: <https://plasticseurope.org/wp-content/uploads/2021/10/2019-Plastics-the-facts.pdf> (accessed on 20 February 2022).
- Mastellone, M.L.; Zaccariello, L. Gasification of polyethylene in a bubbling fluidized bed operated with the air staging. *Fuel* **2013**, *106*, 226–233. [CrossRef]
- Ladanai, S.; Vinterbäck, J. *Global Potential of Sustainable Biomass for Energy*; Report 013; Swedish University of Agricultural Sciences: Uppsala, Sweden, 2009.
- Tumuluru, J.S.; Sokhansanj, S.; Wright, C.T.; Boardman, R.D.; Yancey, N.A. A review on biomass classification and composition, co-firing issues and pretreatment methods. In Proceedings of the American Society of Agricultural and Biological Engineers Annual International Meeting 2011, Louisville, KY, USA, 7–10 August 2011.
- Nam, H.; Capareda, S. Experimental investigation of torrefaction of two agricultural wastes of different composition using RSM. *Energy* **2015**, *91*, 507–516. [CrossRef]
- Balat, M.; Balat, M.; Kirtay, E.; Balat, H. Main routes for the thermo-conversion of biomass into fuels and chemicals. Part 1: Pyrolysis systems. *Energy Convers. Manag.* **2009**, *50*, 3147–3157. [CrossRef]
- Zaccariello, L.; Mastellone, M.L.; D’Amelia, L.I.; Catauro, M.; Morrone, B. Assessment of integration between lactic acid, biogas and hydrochar production in ofmsw plants. *Energies* **2020**, *13*, 6593. [CrossRef]
- Di Lauro, F.; Balsamo, M.; Solimene, R.; Salatino, P.; Montagnaro, F. Hydrothermal liquefaction process to obtain sludge-derived bio-fuels: Setup of the experimental apparatus and preliminary tests. *Chem. Eng. Trans.* **2022**, *92*, 475–480.

12. Zaccariello, L.; Battaglia, D.; Morrone, B.; Mastellone, M.L. Hydrothermal Carbonization: A Pilot-Scale Reactor Design for Bio-waste and Sludge Pre-treatment. *Waste Biomass Valorization* **2022**, *13*, 3865–3876. [[CrossRef](#)]
13. Basu, P. *Biomass Gasification, Pyrolysis and Torrefaction: Practical Design and Theory*, 2nd ed.; Academic Press: London, UK, 2013.
14. Zaccariello, L.; Mastellone, M.L. Gasification of sewage sludge in a bench-scale reactor. *Chem. Eng. Trans.* **2020**, *80*, 175–180.
15. Migliaccio, R.; Brachi, P.; Montagnaro, F.; Papa, S.; Tavano, A.; Montesarchio, P.; Ruoppolo, G.; Urciuolo, M. Sewage Sludge Gasification in a Fluidized Bed: Experimental Investigation and Modeling. *Ind. Eng. Chem. Res.* **2021**, *60*, 5034–5047. [[CrossRef](#)]
16. Montagnaro, F.; Zaccariello, L. Gasification of Spruce Wood Chips in a 1.5 MW_{th} Fluidised Bed Reactor. *Energies* **2022**, *15*, 5883. [[CrossRef](#)]
17. Rios, M.L.V.; González, A.M.; Lora, E.E.S.; del Olmo, O.A.A. Reduction of tar generated during biomass gasification: A review. *Biomass Bioenergy* **2018**, *108*, 345–370. [[CrossRef](#)]
18. Lopez, G.; Artetxe, M.; Amutio, M.; Alvarez, J.; Bilbao, J.; Olazar, M. Recent advances in the gasification of waste plastics. A critical overview. *Renew. Sustain. Energy Rev.* **2018**, *82*, 576–596. [[CrossRef](#)]
19. Mishra, R.; Singh, E.; Kumar, A.; Ghosh, A.; Lo, S.L.; Kumar, S. Co-gasification of solid waste and its impact on final product yields. *J. Clean. Prod.* **2022**, *374*, 133989. [[CrossRef](#)]
20. Ünlü, N.; Özdoğan, S. Entrained flow Co-gasification of torrefied biomass and coal. *Energy* **2023**, *263*, 125864. [[CrossRef](#)]
21. Chai, Y.; Gao, N.; Wang, M.; Wu, C. H₂ production from co-pyrolysis/gasification of waste plastics and biomass under novel catalyst Ni–CaO–C. *Chem. Eng. J.* **2020**, *382*, 122947. [[CrossRef](#)]
22. Jakab, E.; Várhegyi, G.; Faix, O. Thermal decomposition of polypropylene in the presence of wood-derived materials. *J. Anal. Appl. Pyrolysis* **2000**, *56*, 273–285. [[CrossRef](#)]
23. Lopez, G.; Artetxe, M.; Amutio, M.; Bilbao, J.; Olazar, M. Effect of polyethylene co-feeding in the steam gasification of biomass in a conical spouted bed reactor. *Fuel* **2015**, *153*, 393–401. [[CrossRef](#)]
24. Moghadam, R.A.; Yusup, S.; Uemura, Y.; Chin, B.L.F.; Lam, H.L.; Al Shoaibi, A. Syngas production from palm kernel shell and polyethylene waste blend in fluidized bed catalytic steam co-gasification process. *Energy* **2014**, *75*, 40–44. [[CrossRef](#)]
25. Block, C.; Ephraim, A.; Weiss-Hortala, E.; Minh, D.P.; Nzihou, A.; Vandecasteele, C. Co-pyrogasification of plastics and biomass, a review. *Waste Biomass Valor.* **2019**, *10*, 483–509. [[CrossRef](#)]
26. Smoliński, A.; Wojtacha-Rychter, K.; Król, M.; Magdziarczyk, M.; Polański, J.; Howaniec, N. Co-gasification of refuse-derived fuels and bituminous coal with oxygen/steam blend to hydrogen rich gas. *Energy* **2022**, *254*, 124210. [[CrossRef](#)]
27. Ruoppolo, G.; Ammendola, P.; Chirone, R.; Miccio, F. H₂-rich syngas production by fluidized bed gasification of biomass and plastic fuel. *Waste Manag.* **2012**, *32*, 724–732. [[CrossRef](#)] [[PubMed](#)]
28. Déparrois, N.; Singh, P.; Burra, K.G.; Gupta, A.K. Syngas production from co-pyrolysis and co-gasification of polystyrene and paper with CO₂. *Appl. Energy* **2019**, *246*, 1–10. [[CrossRef](#)]
29. Li, J.; Burra, K.R.G.; Wang, Z.; Liu, X.; Gupta, A.K. Co-gasification of high-density polyethylene and pretreated pine wood. *Appl. Energy* **2021**, *285*, 116472. [[CrossRef](#)]
30. Mastellone, M.L.; Zaccariello, L.; Arena, U. Co-gasification of coal, plastic waste and wood in a bubbling fluidized bed reactor. *Fuel* **2010**, *89*, 2991–3000. [[CrossRef](#)]
31. Channiwala, S.A.; Parikh, P.P. A unified correlation for estimating HHV of solid, liquid and gaseous fuels. *Fuel* **2002**, *81*, 1051–1063. [[CrossRef](#)]
32. Han, S.W.; Lee, J.J.; Tokmurzin, D.; Lee, S.H.; Nam, J.Y.; Park, S.J.; Ra, H.W.; Mun, T.Y.; Yoon, S.J.; Yoon, S.M.; et al. Gasification characteristics of waste plastics (SRF) in a bubbling fluidized bed: Effects of temperature and equivalence ratio. *Energy* **2022**, *238*, 121944. [[CrossRef](#)]
33. Chernov, V.; Thomson, M.J.; Dworkin, S.B.; Slavinskaya, N.A.; Riedel, U. Soot formation with C₁ and C₂ fuels using an improved chemical mechanism for PAH growth. *Combust. Flame* **2014**, *161*, 592–601. [[CrossRef](#)]
34. Karl, J.; Pröll, T. Steam gasification of biomass in dual fluidized bed gasifiers: A review. *Renew. Sustain. Energy Rev.* **2018**, *98*, 64–78. [[CrossRef](#)]
35. Wang, Z.; Burra, K.G.; Zhang, M.; Li, X.; He, X.; Lei, T.; Gupta, A.K. Syngas evolution and energy efficiency in CO₂-assisted gasification of pine bark. *Appl. Energy* **2020**, *269*, 114996. [[CrossRef](#)]
36. Kartal, F.; Özveren, U. Energy and exergy analysis of entrained bed gasifier/GT/Kalina cycle model for CO₂ co-gasification of waste tyre and biochar. *Fuel* **2023**, *331*, 125943. [[CrossRef](#)]
37. Sahu, P.; Vairakannu, P. CO₂ based co-gasification of printed circuit board with high ash coal. *Energy* **2023**, *263*, 125977. [[CrossRef](#)]
38. Pinto, F.; André, R.; Miranda, M.; Neves, D.; Varela, F.; Santos, J. Effect of gasification agent on co-gasification of rice production wastes mixtures. *Fuel* **2016**, *180*, 407–416. [[CrossRef](#)]
39. Cheng, Y.; Thow, Z.; Wang, C.H. Biomass gasification with CO₂ in a fluidized bed. *Powder Technol.* **2016**, *296*, 87–101. [[CrossRef](#)]
40. Mastellone, M.L.; Zaccariello, L. Metals flow analysis applied to the hydrogen production by catalytic gasification of plastics. *Int. J. Hydrogen Energy* **2013**, *38*, 3621–3629. [[CrossRef](#)]
41. Arena, U.; Zaccariello, L.; Mastellone, M.L. Fluidized bed gasification of waste-derived fuels. *Waste Manag.* **2010**, *30*, 1212–1219. [[CrossRef](#)]

42. Hernández, J.J.; Ballesteros, R.; Aranda, G. Characterisation of tars from biomass gasification: Effect of the operating conditions. *Energy* **2013**, *50*, 333–342. [[CrossRef](#)]
43. Abu El-Rub, Z.; Bramer, E.A.; Brem, G. Experimental comparison of biomass chars with other catalysts for tar reduction. *Fuel* **2008**, *87*, 2243–2252. [[CrossRef](#)]

Disclaimer/Publisher’s Note: The statements, opinions and data contained in all publications are solely those of the individual author(s) and contributor(s) and not of MDPI and/or the editor(s). MDPI and/or the editor(s) disclaim responsibility for any injury to people or property resulting from any ideas, methods, instructions or products referred to in the content.